

ARTICLE

OPEN



Identification of novel therapeutic targets for cognitive performance and associations with brain health

Lu-Yang Zhang^{1,2,3,4}, Yu-Xin Liu^{1,2,3,4}, Yun-Hui Chu^{1,2,3}, Yun-Fan You^{1,2,3}, Luo-Qi Zhou^{1,2,3}, Sheng Yang^{1,2,3}, Ming-Hao Dong^{1,2,3}, Hang Zhang^{1,2,3}, Xiao-Wei Pang^{1,2,3}, Lian Chen^{1,2,3}, Li-Fang Zhu^{1,2,3}, Jun Xiao^{1,2,3}, Ke Shang^{1,2,3}, Wei Wang^{1,2,3}, Chuan Qin^{1,2,3} and Dai-Shi Tian^{1,2,3}

© The Author(s) 2025

Cognitive dysfunction poses a significant challenge in clinical practice, but currently available drugs mainly address symptoms and have limited effectiveness in treating cognitive dysfunction associated with various neurological disorders. Mendelian randomization (MR) and colocalization analyses were conducted to explore the causal associations between 4302 druggable genes with blood and brain cis-expression quantitative trait loci (eQTLs) and cognitive performance. The causal effects of candidate druggable genes on brain structure and neurological diseases were assessed to gain insights into the underlying mechanisms. Among over 4000 druggable genes, our study identified causal associations between 72 druggable genes (41 blood eQTLs and 31 brain eQTLs) and cognitive performance. Thirteen eQTLs (six in blood: *ERBB3*, *SPEG*, *ATP2A1*, *GDF11*, *CYP2D6*, *GANAB*; seven in brain: *ERBB3*, *DPYD*, *TAB1*, *WNT4*, *CLCN2*, *PPM1B*, *CAMKIV*) were identified as candidate druggable genes for cognitive performance. Notably, both blood and brain eQTLs of *ERBB3* were negatively associated with cognitive performance (blood: OR = 0.933, 95% CI 0.911–0.956, *p*-value = 9.69E-09; brain: OR = 0.782, 95% CI 0.718–0.852, *p*-value = 2.13E-08). Moreover, these candidate druggable genes exhibited causal effects on both brain structure and neurological diseases. Our integrative analysis provides genetic evidence supporting candidate therapeutic targets for improving cognitive performance and treating neurological diseases. Furthermore, it sheds light on the possible mechanisms by which these targets affect brain structures. This finding suggested that these identified druggable genes, particularly *ERBB3* and *CYP2D6*, hold promise as potential drug targets for enhancing cognitive performance.

Translational Psychiatry (2025)15:214; <https://doi.org/10.1038/s41398-025-03437-w>

INTRODUCTION

Cognitive dysfunction poses a significant challenge in clinical practice, with a complex etiology encompassing psychiatric, cerebrovascular, and neurodegenerative diseases such as Alzheimer's disease (AD), as well as other medical disorders such as brain tumors, head trauma, intracranial infection, alcohol or drug abuse, along with natural aging [1–4]. This condition manifests across various cognitive domains, presenting as amnesia, aphasia, visuospatial deterioration, executive dysfunction, attention deficits [5], and dementia or disability in severe cases, imposing a substantial economic burden on individuals, caregivers, and society levels. Despite its impact, effective clinical treatments remain elusive. Currently, only a few drugs, such as cholinesterase inhibitors and NMDA inhibitors, are approved for cognitive dysfunction. However, these drugs primarily target symptoms and cannot cure or delay disease progression. Moreover, ongoing experimental therapeutic modalities targeting AD mechanisms and pathological changes, including anti-A β and anti-Tau therapies, neuroinflammatory therapy, neuroprotective agents, and brain stimulation therapy [6], exhibit limited generalizability to cognitive dysfunction arising from diverse neurological

disorders. Furthermore, not all clinical trials have achieved favorable outcomes, as seen with verubecstat, semagacestat, semorinemab [7–9]. Therefore, it is urgent to identify novel and effective therapeutic targets to address cognitive impairment.

Cognitive impairment is associated with various structural alterations in the brain, including progressive cortical thinning [10], widespread grey matter atrophy in cortical and subcortical regions [11], and white matter damage [12, 13]. White matter lesions can be detected non-invasively by diffusion tensor imaging (DTI) and are characterized by three phenotypes: white matter hyperintensities (WMH), fractional anisotropy (FA), and mean diffusivity (MD) [14]. Additionally, the structural-functional connectivity of the cortex, such as the medial temporal lobe and precuneus, also plays an important role in cognition [15, 16]. Considering the impact cognitive impairment has on multiple brain structures, it becomes evident that new drug targets can be developed to address these damages.

Mendelian randomization (MR) serves as an alternative approach to randomized controlled trials to assess the causality between exposures and relevant clinical outcomes [17]. Drug target MR analysis, which is increasingly applied for drug target

¹Department of Neurology, Tongji Hospital, Tongji Medical College and State Key Laboratory for Diagnosis and Treatment of Severe Zoonotic Infectious Diseases, Huazhong University of Science and Technology, Wuhan 430030, China. ²Hubei Key Laboratory of Neural Injury and Functional Reconstruction, Huazhong University of Science and Technology, Wuhan 430030, China. ³Key Laboratory of Vascular Aging, Ministry of Education, Tongji Hospital of Tongji Medical College, Huazhong University of Science and Technology, Wuhan 430030, China. ⁴These authors contributed equally: Lu-Yang Zhang, Yu-Xin Liu. email: chuanqin@tjh.tjmu.edu.cn; tiands@tjh.tjmu.edu.cn

Received: 27 May 2024 Revised: 19 May 2025 Accepted: 12 June 2025
Published online: 25 June 2025

screening, utilizes genetic variants situated within the genomic region of drug target genes by integrating genetic (i.e., genome-wide association study, GWAS) and transcriptomic data (i.e., expression quantitative trait locus, eQTL) to emulate the long-term regulation of gene expression [18]. The druggable genome has been summarized by integrating the human disease and biomarker GWAS data along with a list of genes encoding druggable human proteins [19]. Previous drug target MR analyses have effectively utilized the druggable genome data, uncovering novel drug targets for various disorders such as Parkinson's disease (PD), COVID-19, aortic aneurysms, and AD [20–23]. However, few studies have explored the associations of a broad spectrum of drug targets with cognitive performance and brain health.

Hence, our study employs MR and colocalization analyses to identify potential targets for cognitive dysfunction. We also assess the causal relationships between these identified druggable genes and brain structure to elucidate the mechanisms by which these genes contribute to the pathogenesis of cognitive dysfunction, with the aim of unveiling new targets for drug development to enhance cognitive performance and delay cognitive decline.

METHODS

Study design

This study aimed to identify therapeutic targets relevant to cognitive performance. The overall workflow was shown in Fig. 1. Firstly, a total of 4302 drug target genes were extracted from the druggable genome and screened for instrument selection [19]. Subsequently, a two-sample MR analysis was performed to evaluate the causal associations between blood and brain druggable eQTLs and cognitive performance. Regarding the drug target genes causally associated with cognitive performance after multiple comparisons, we conducted colocalization analysis to confirm that cognitive performance and the eQTLs may share causal genetic variants. To explore the associations between candidate druggable genes and specific cognitive function domains, MR analyses were performed for fluid intelligence scores, memory performance, and reaction time. The causal associations between candidate druggable genes and brain structure were further evaluated. A total of 274 brain structure imaging phenotypes, including 6 different categories (FA, MD, cortical volume, cortical area, cortical thickness, and subcortical volume), were evaluated. Finally, we assessed the causal impact of the candidate druggable genes on different neurological diseases.

Druggable genome data and eQTL datasets

In accordance with the druggable genome, there were 4302 druggable genes located on the autosomal chromosomes (chromosome 1–22) annotated with HGNC gene symbols (Table S1) [19]. The blood eQTL data were from the eQTLGen Consortium (<https://eqtlgen.org/>), where the *cis*-eQTL data were obtained from peripheral blood samples of European ancestry individuals ($N = 31,684$) [24]. The brain eQTL dataset was obtained from the PsychENCODE Consortium (<http://resource.psychencode.org>), which contained 1387 prefrontal cortex and primarily European ancestry samples [25].

Three key assumptions in MR must be met to ensure the validity of instrumental variables (IVs): (1) IVs are directly related to the exposure, (2) IVs are independent of confounding factors, and (3) IVs are independent of the outcome [26]. First, *cis*-eQTL data from blood and brain tissues were used as proxies for the effect of drug target genes. To extract genetic variants closely related to drug target gene expression, the *cis*-eQTL located within 1 Mb downstream or upstream of the region of the drug target genes was screened. Significant *cis*-eQTL results [false discovery rate (FDR) < 0.05] with F -statistic (calculated by the formula: $F\text{-statistic} = \beta/\text{se}^2 > 10$) were selected initially [27]. Subsequently, linkage disequilibrium (LD) was assessed among the genetic variants based on the 1000 Genomes European reference. The independent genetic variants without LD ($r^2 < 0.001$ within a 10,000 kb window) were retained as the IVs in the MR analysis. Further details are presented in the original publications [24, 25] and Table S2.

In addition, protein quantitative trait loci (pQTL) data of candidate drug targets were extracted for MR analysis as validation. The GWAS summary-level statistics on circulating plasma protein were extracted

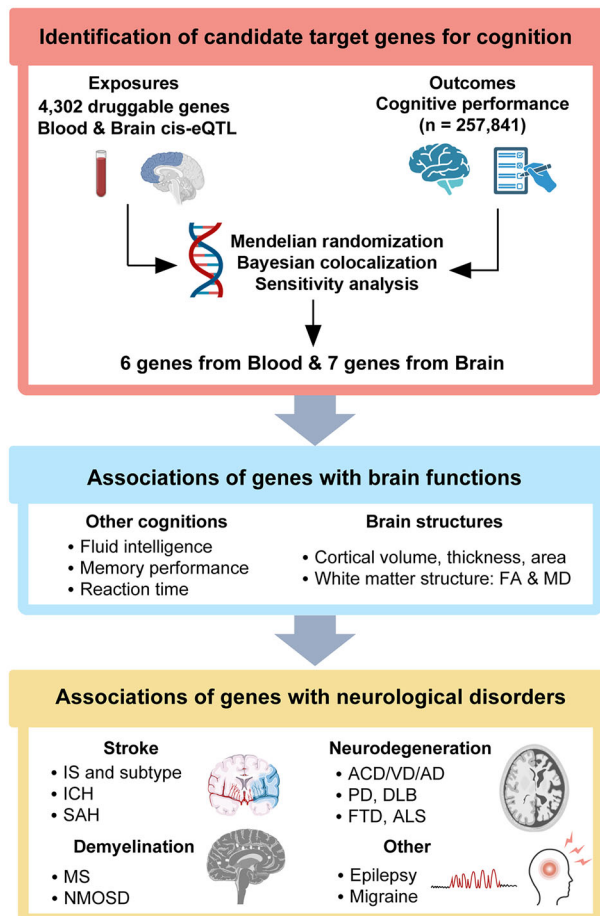


Fig. 1 The design flow of the study. First, we used eQTLs from brain tissue and blood, intersecting with druggable genes, to acquire instrumental variables. Second, MR and colocalization analyses were conducted to explore the causal associations of blood and brain eQTLs with cognitive performance. Then, we evaluated the causal relationships between candidate druggable genes and cognitive function domains and brain structure, aiming to explore potential mechanisms. Finally, we assessed the causal impact of the candidate druggable genes on various neurological diseases. ACD all-cause dementia, ALS amyotrophic lateral sclerosis, DLB dementia with Lewy bodies, eQTL expression quantitative trait loci, FA fractional anisotropy, FTD frontotemporal dementia, ICH intracerebral hemorrhage, IS ischemic stroke, MD mean diffusivity, MS multiple sclerosis, NMOSD neuromyelitis optica spectrum disorder, PD Parkinson's disease, SAH subarachnoid hemorrhage, VaD vascular dementia.

from the deCODE consortium (<https://www.decode.com/summarydata/>). The detailed description of the datasets is available in the original publication [28] and Table S2. This study included the proteins with pQTLs available at the genome-wide significance level ($p\text{-value} < 5\text{E}-08$) in two-sample MR analysis.

GWAS of cognition function outcomes

Several cognitive function outcomes included in the present study were as follows: cognitive performance extracted from a recent GWAS meta-analysis ($N = 257,841$) combining data from UK Biobank (UKB) fluid intelligence verbal-numerical reasoning scores and the Cognitive Genomics Consortium neuropsychological test data [29]; fluid intelligence score measured as the number of correct answers on a 13-question test utilizing UKB data ($N = 149,051$) [30]; memory performance measured as the total number of errors on a pairs matching test conducted without time limit using UKB data ($N = 112,067$) [31]; mean reaction time for four matching trials in milliseconds using the UKB data ($N = 330,069$) [32]. A larger number of memory performance scores or reaction time indicates poorer

cognition. The details of the cognitive function GWAS datasets were provided in Table S3.

GWAS of brain structure imaging measurements

The corresponding genetic variants linked to brain structure were obtained from a GWAS meta-analysis conducted by Smith et al. [33]. They undertook a GWAS of brain imaging phenotypes in UKB, comprising regional and tissue volume, regional and tissue intensity, and cortical thickness, with a total of 39,691 brain imaging samples [33]. In this study, the categories comprised FA, MD, cortical volume (CV), cortical area (CA), cortical thickness (CTH), and subcortical volume (sub-CV). Among others, FA indicates the directionality of water diffusion in DTI, with 0 representing unrestricted water flow and 1 representing most directionally restricted flow, which indicates high myelination [34]. MD measures the average rate of water diffusion in any direction, reflecting an inverse pattern to FA [35]. They both reflect the tissue integrity. Higher MD and lower FA can be found in the pathological white matter [36]. The original data can be accessible for downloading via the following website: <https://openwin.ox.ac.uk/ukbiobank/big40/>. Detailed information regarding the GWAS datasets was shown in Table S4.

GWAS of neurological diseases

We extracted genetic variants of any stroke (AS, 40,585 cases and 406,111 controls), ischemic stroke (IS, 34,217 cases) and its subtypes from the MEGASTROKE consortium, including large artery atherosclerosis stroke (LAS, 4373 cases), cardioembolic stroke (CES, 7193 cases), and small vessel stroke (SVS, 5386 cases) [37]. For intracerebral hemorrhage (ICH, 1687 cases), subarachnoid hemorrhage (SAH, 1338 cases), any dementia (ACD, 5933 cases), vascular dementia (VaD, 881 cases), dementia due to Parkinson's disease (PDD, 267 cases), and migraine (8547 cases), GWAS data were derived from the FinnGen consortium [38]. The genetic data of dementia with Lewy bodies (DLB) and frontotemporal dementia (FTD) were extracted from a recent GWAS by Chia et al., involving 2591 cases and 4027 controls [39], and Van Deerlin, with 515 cases and 2509 controls [40], respectively. For AD, PD, and amyotrophic lateral sclerosis (ALS), we utilized the corresponding GWAS data from the International Genomics of Alzheimer's Project (21,982 cases and 41,944 controls) [41], the International Parkinson's Disease Genomics Consortium (33,674 cases and 449,056 controls) [42], and the ALS Variant Server (20,806 cases and 59,804 controls) [43]. Furthermore, another extensive GWAS involving 75,024 clinically diagnosed AD and AD-by-proxy cases, along with 397,844 controls, was also utilized [44]. Genetic association estimates for multiple sclerosis (MS), MS severity, and epilepsy were obtained respectively from the International Multiple Sclerosis Genetics Consortium (47,429 cases and 68,374 controls for MS, 12,584 cases for MS severity) [45, 46] and the International League Against Epilepsy consortium (15,212 cases and 2,9677 controls) [47]. The genetic variants associated with neuromyelitis optica spectrum disorder (NMOSD) were derived from an extensive GWAS database, comprising 215 cases diagnosed with NMOSD and 1244 controls. This included 132 with aquaporin-4 antibody-positive NMOSD (AQP4⁺NMOSD), 83 with aquaporin-4 antibody-negative NMOSD (AQP4⁻NMOSD) [48]. For external validation, summary statistics were included SAH (1693 cases and 471,562 controls) [49], ALS (22,040 cases and 62,644 controls) [43], epilepsy (N = 407,746) [50], and DLB (1393 cases and 2271 controls) [51]. All these GWAS were conducted on individuals of European ancestry, except for the epilepsy dataset. Detailed descriptions of the datasets can be found in Table S5.

Two-sample mendelian randomization analysis

All MR analyses in this study were carried out via TwoSampleMR R package with R version 4.0.3 [30]. The impact of druggable genes on outcomes was assessed using the Wald ratio method for single-IV and the inverse variance weighted (IVW) method for cases with two or more IVs. This method meta-analyzed the Wald ratios for each IV, assuming balanced pleiotropy [52]. If no evidence of heterogeneity was detected, a fixed-effects IVW method was applied. In the presence of heterogeneity, a multiplicative random-effects IVW method was used to estimate the causal effect. As further analyses, simple mode, MR-Egger, weighted mode, and weighted median methods were performed [53–55]. Heterogeneity and pleiotropy analyses were carried out using the Cochran Q test and MR-Egger intercept test, respectively [54]. Regarding multiple comparisons, the Bonferroni correction was applied (adjusted *p*-value = 0.05/X/Y, where X represented the number of exposures and Y represented the number of

outcomes). A suggestive association between exposure and outcome was defined as a *p*-value between the adjusted *p*-value and 0.05. Additionally, Steiger filtering analysis was conducted to explore the direction of causal relationships of exposures with outcomes, aiming to exclude the possibility of reverse causality [56].

Bayesian colocalization analysis

Concerning the significant druggable genes identified in the primary drug target MR analyses for cognitive performance, colocalization analysis was subsequently carried out using R package *coloc* [57] with default prior probabilities: $P_1 = 1 \times 10^{-4}$, $P_2 = 1 \times 10^{-4}$, $P_{12} = 1 \times 10^{-5}$. P_1 , P_2 , and P_{12} represent the prior probabilities that a given SNP in the test region is significantly associated with gene expression, the outcome, or both, respectively. The colocalization analysis employed the approximate Bayes factor (ABF) computation to derive posterior probabilities (PP) based on five assumptions, which are: (1) neither trait has a causal single-nucleotide polymorphism (SNP) (H0); (2) only trait 1 has the causal SNP (H1); (3) only trait 2 has the causal SNP (H2); (4) both traits are associated but with different causal SNPs (H3); (5) both traits are associated and share the same causal SNP (H4) [58]. A PPH4 > 0.8 was used to indicate high-support evidence for colocalization, while PPH4 values between 0.7 and 0.8 were considered as medium-support evidence for colocalization.

White matter tractography

We extracted DTI traits of brain from the Consortium for Reliability and Reproducibility, which has aggregated resting state fMRI and diffusion imaging data from laboratories around the world and has shared the data via the International Neuroimaging Data-sharing Initiative, providing an open data resource for the imaging community (https://fcon_1000.projects.nitrc.org/indi/CoRR/html/index.html). Then white matter tracts were separated using DSI studio (<http://dsi-studio.labsolver.org>), the color of different tracts refers to the z value (ratio of β and se) of druggable genes to the FA, MD of white matter.

RESULTS

Significant druggable genes for cognitive performance

We used eQTLs from both brain and blood, intersecting with druggable genes to acquire druggable eQTLs. In total, 2637 and 2898 target genes, after clumping with at least one IV, were retained in blood eQTLs and brain eQTLs, respectively (Tables S6, S7). 41 blood eQTLs and 31 brain eQTLs as potential drug targets for cognitive performance were identified using either the Wald ratio or the IVW method (blood: adjusted *p*-value = 0.05/2637 = 1.89E-05; brain: adjusted *p*-value = 0.05/2898 = 1.72E-05, Fig. 2A). The IVs for significant expression and full MR results were presented in Tables S8, S9. No heterogeneity or pleiotropy was identified in the sensitivity analyses (all *p*-values > 0.05, Table S10).

Colocalization analysis

Colocalization analysis identified six blood eQTLs (*ERBB3*, *SPEG*, *ATP2A1*, *GDF11*, *CYP2D6*, *GANAB*) and seven brain eQTLs (*ERBB3*, *DPYD*, *TAB1*, *WNT4*, *CLCN2*, *PPM1B*, *CAMKV*) as candidate druggable genes, providing evidence of genetic colocalization with cognitive performance (Table 1 and Figures S1, S2). Among them, *GANAB*, *PPM1B* and *CAMKV* provided medium-support evidence for colocalization (0.7 < PPH4 < 0.8), while the remaining genes showed high-support evidence for colocalization (PPH4 > 0.8). Of note, the probability ratio [PPH4/(PPH3 + PPH4)] of *ERBB3* in both blood and brain eQTL datasets reached 99%, further validating its colocalization with cognitive performance (Table 1 and Fig. 2B) [59].

Association between candidate druggable genes and cognitive function domains

All candidate druggable genes were causally associated with cognitive performance, among which *CYP2D6*, *SPEG* in the blood and *CLCN2*, *DPYD* in the brain were beneficial for enhancing cognition, while the others were on the contrary (Table S11 and

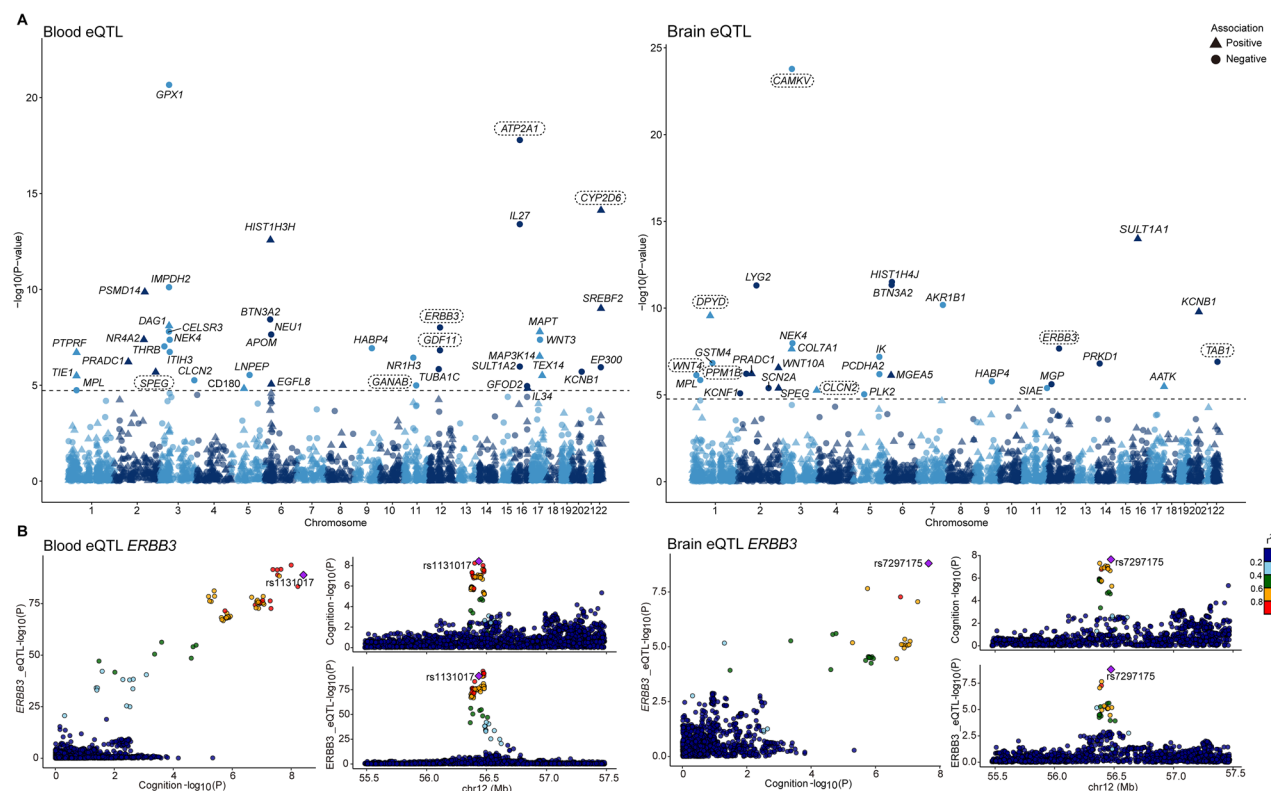


Fig. 2 Manhattan plots and locus zoom plot for associations of druggable genes with cognitive performance in MR analysis. **A** Manhattan plots for associations of druggable genes with cognitive performance in MR analysis. The left and right panels show associations of druggable genes from blood eQTLs and brain eQTLs with cognitive performance, respectively. Labeled genes refer to MR findings with p -value < 1.896E-05 (blood eQTLs) or p -value < 1.725E-05 (brain eQTLs). Triangular plots indicate the positive effect of the druggable gene on the outcome; round plots indicate the negative effect of the druggable gene on the outcome. Candidate druggable genes with colocalization evidence were framed. Results are plotted according to the gene start position. **B** Regional locus zoom plot of the associations of SNPs with *ERBB3* locus. The left panel shows the associations of blood eQTL *ERBB3* with cognitive performance; The right panel shows the associations of brain eQTL *ERBB3* with cognitive performance.

Table 1. Mendelian randomization analysis and colocalization of druggable genes and cognitive performance.

Dataset	Druggable genes	MR analysis		Colocalization Analysis	
		OR (95%CI)	P value	PP.H4	PP.H4/PP.H3 + PP.H4
Blood eQTL	<i>ERBB3</i>	0.933 (0.911–0.956)	9.69E-09	0.992	0.992
	<i>SPEG</i>	1.082 (1.047–1.117)	2.07E-06	0.950	0.955
	<i>ATP2A1</i>	0.818 (0.783–0.856)	1.63E-18	0.926	0.926
	<i>GDF11</i>	0.847 (0.797–0.901)	1.50E-07	0.887	0.888
	<i>CYP2D6</i>	1.049 (1.037–1.062)	7.55E-15	0.837	0.837
	<i>GANAB</i>	0.956 (0.938–0.976)	1.02E-05	0.753	0.765
Brain eQTL	<i>ERBB3</i>	0.782 (0.718–0.852)	2.13E-08	0.997	0.997
	<i>DPYD</i>	1.599 (1.382–1.850)	2.76E-10	0.938	0.973
	<i>TAB1</i>	0.804 (0.741–0.872)	1.24E-07	0.935	0.950
	<i>WNT4</i>	0.902 (0.866–0.940)	7.28E-07	0.929	0.930
	<i>CLCN2</i>	1.173 (1.095–1.257)	5.47E-06	0.928	0.979
	<i>PPM1B</i>	0.712 (0.623–0.814)	6.05E-07	0.759	0.906
	<i>CAMKV</i>	0.489 (0.426–0.561)	1.65E-24	0.738	0.743

PP indicates posterior probability.

H3: both traits are associated, but with different causal variants.

H4: both traits are associated and share a single causal variant.

CI confidence interval; MR Mendelian randomization; OR odds ratio.

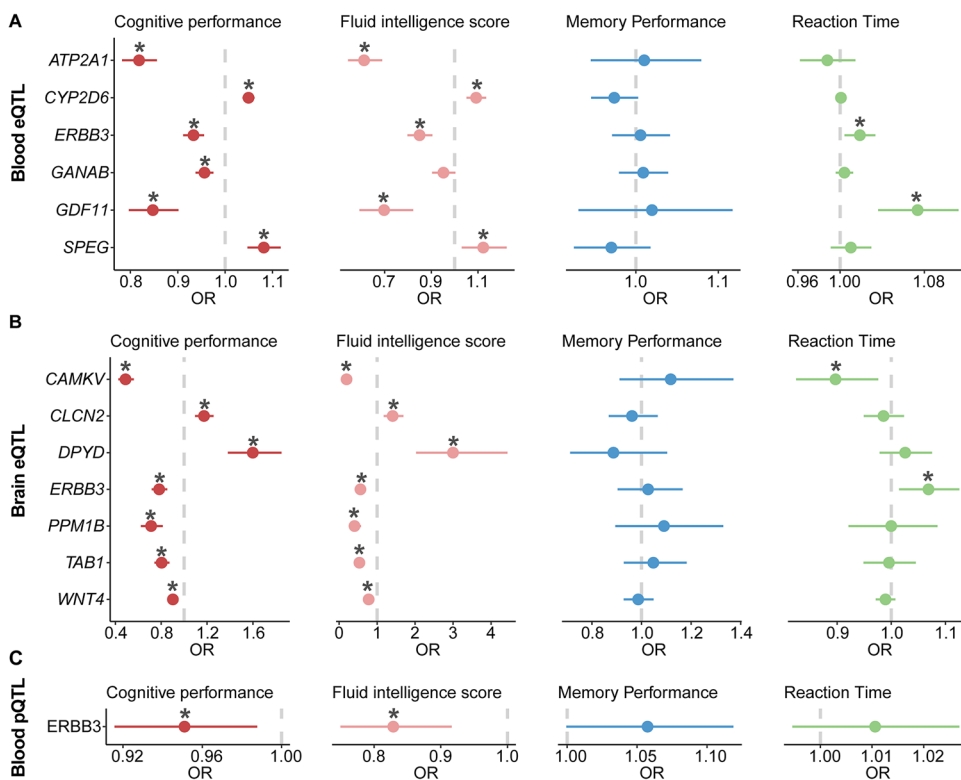


Fig. 3 Association between candidate druggable genes and cognitive function. Forest plot of Mendelian randomization effect estimates and 95% CI for the genetic proxied candidate druggable genes and cognitive function. Causal associations that remained significant after Bonferroni-correction were marked with an asterisk (* p -value < 0.0125). **A** Results for blood eQTLs; **B** Results for brain eQTLs; **C** Results for blood pQTLs of ERBB3. All candidate druggable genes except GANAB were significantly associated with fluid intelligence score. Moreover, GDF11 and CAMKV demonstrated a significant association with reaction time. Both blood and brain eQTLs of ERBB3 were positively significant associated with reaction time. Additionally, blood pQTL ERBB3 were significantly associated with both cognitive performance and fluid intelligence score consistent with the eQTL results. eQTL expression quantitative trait loci, OR odds ratio.

Fig. 3A, B). Fluid intelligence, memory performance, and reaction time, deemed as domains of cognitive performance, were also analyzed (adjusted p -value = 0.05/4 = 0.0125). Specifically, the association directionality of candidate druggable genes with fluid intelligence exhibited similarity with cognitive performance except GANAB. ERBB3, GDF11 in the blood and ERBB3, CAMKV in the brain were causally associated with reaction time, while none was found relevant to memory performance (GDF11: OR = 1.073, 95% CI 1.036–1.112, p -value = 9.02E-05; CAMKV: OR = 0.897, 95% CI 0.825–0.976, p -value = 0.012; blood ERBB3: OR = 1.019, 95% CI 1.004–1.034, p -value = 0.011; brain ERBB3: OR = 1.069, 95% CI 1.014–1.126, p -value = 0.012; Table S11 and Fig. 3A, B).

Additionally, during our replication, blood pQTL ERBB3 from the deCODE consortium was significantly associated with both cognitive performance (OR = 0.951, 95% CI 0.916–0.988, p -value = 9.32E-03) and fluid intelligence score (OR = 0.829, 95% CI 0.750–0.916, p -value = 2.48E-04), consistent with the eQTL result (Table S11 and Fig. 3C). No heterogeneity or pleiotropy was identified in the sensitivity analyses (all p -values > 0.05, Table S12).

Association between candidate druggable genes and brain structure

We further investigated the associations between candidate druggable genes and brain structure. Among candidate druggable genes, blood eQTLs ERBB3, ATP2A1, and GANAB had not been found as instrumental variables in GWAS of brain structure imaging measurements conducted in the analysis.

Candidate druggable genes and white matter structure

The causal associations between candidate druggable genes and 54 white matter structure imaging phenotypes (FA and MD) were

further evaluated. Under the Bonferroni correction (adjusted p -value = 0.05/27 = 1.85E-03), significant causal associations are as follows: in the brain, nine fiber phenotypes were associated with ERBB3, one with CLCN2 and CAMKV, respectively; in the blood, ten fiber phenotypes were associated with GDF11 and one with CYP2D6. Among these white matter fibers, ERBB3 was positively associated with FA in the right uncinate fasciculus (OR = 1.663, 95% CI 1.307–2.115, p -value = 3.44E-05), which is a frontotemporal connection. This association was further validated in the relationships with MD (OR = 0.647, 95% CI 0.508–0.823, p -value = 3.84E-04). Of note, we found that genetically determined higher ERBB3 protein levels were associated with higher FA values of right corticospinal tract (OR = 1.196, 95% CI 1.075–1.331, p -value = 9.83 E-04), and lower MD values of left parahippocampal part of cingulum (OR = 0.840, 95% CI 0.755–0.935, p -value = 1.35E-03), served as supplementary information to the genetic role of ERBB3 to white matter structure.

Additionally, we found that blood eQTL CYP2D6 exerted positive effects on FA in the left anterior thalamic radiation (OR = 1.057, 95% CI 1.021–1.093, p -value = 1.67E-03), which connects thalamus and frontal lobe. Higher expression of GDF11 in the blood was associated with lower MD values in multiple white matter tracts, such as both sides of inferior fronto-occipital fasciculus (left: OR = 0.691, 95% CI 0.582–0.821, p -value = 2.71E-05; right: OR = 0.691, 95% CI 0.582–0.822, p -value = 2.75E-05), and also both sides of inferior longitudinal fasciculus (left: OR = 0.745, 95% CI 0.627–0.886, p -value = 8.37E-04; right: OR = 0.730, 95% CI 0.614–0.867, p -value = 3.41E-04). The detailed results of candidate druggable genes and 57 imaging measures of white matter structure were shown in Fig. 4, Fig. 5A, Figure S3, and Table S13.

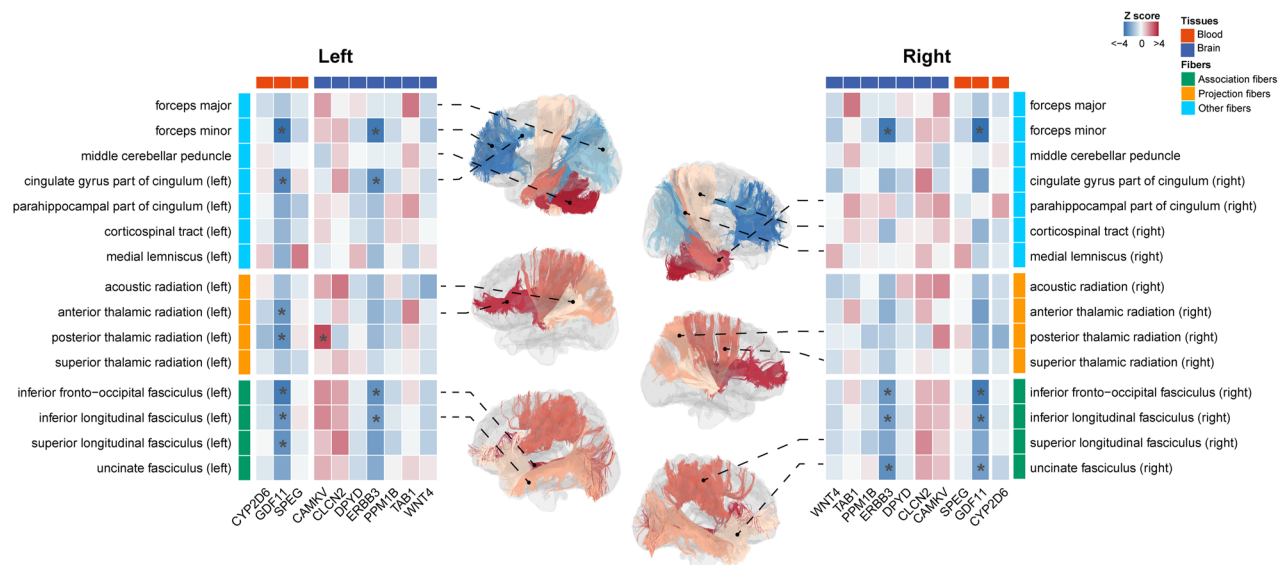


Fig. 4 Association between candidate druggable genes and white matter structure. The heatmap visually represents the causal effects of candidate druggable genes on white matter MD, which was presented by z-score. Causal associations that remained significant after Bonferroni-correction were marked with an asterisk (* p -value < 1.85E-03). The rows represent the 27 white matter regions, and the columns represent the 10 candidate druggable genes. eQTL expression quantitative trait loci, MD mean diffusivity.

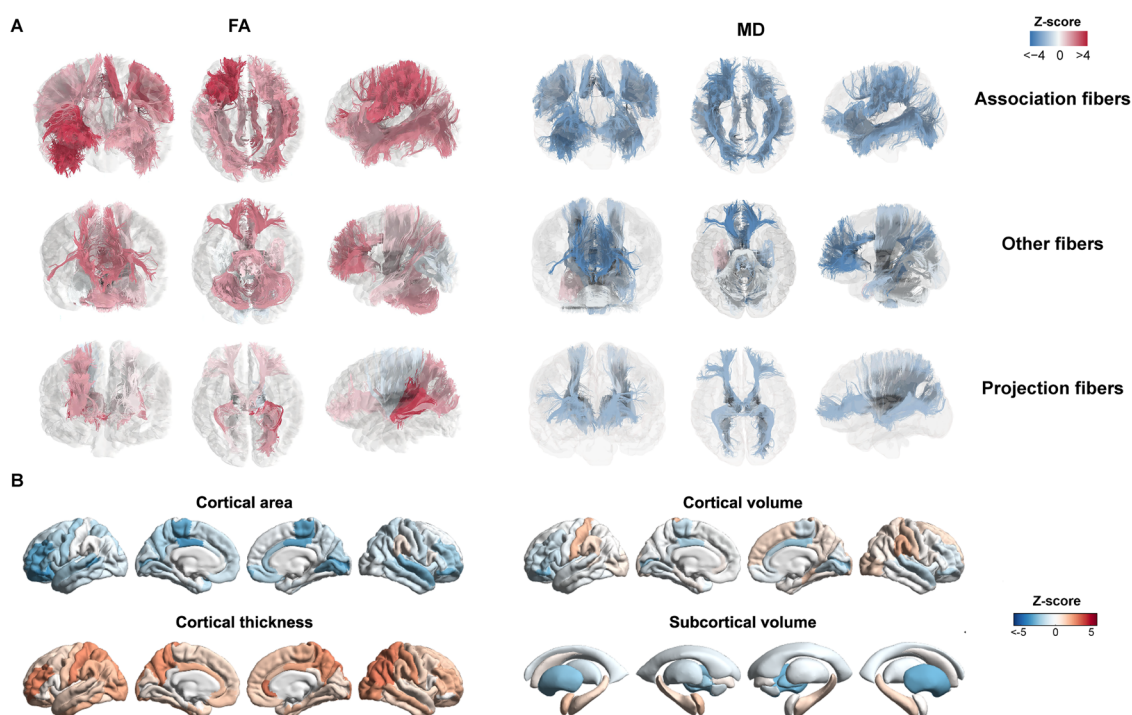


Fig. 5 The causal effects of brain eQTL ERBB3 on brain structure. **A** Genetically predicted ERBB3 associated white matter MRI metrics. White matter maps representing z-scores of associations between ERBB3 and main white matter tracts (Bonferroni-corrected p -value < 1.85E-03). Other fibers included the main brainstem, limbic, and commissural fibers. **B** Genetically predicted ERBB3 associated cortical and subcortical regional MRI metrics. Cortical and subcortical maps representing z-scores of associations between ERBB3 and regional MRI metrics (Bonferroni-corrected p -value for cortical structures < 1.47E-03; bonferroni-corrected p -value for subcortical structures < 6.25E-03). CA cortical area, CTH cortical thickness, CV cortical volume, FA fractional anisotropy, MD mean diffusivity, Sub-CV subcortical volume.

Candidate druggable genes and cortical, subcortical structure
Then, the causal relationships between candidate druggable genes and cortical structure (CA, CV, and CTH) were assessed using MR analysis (adjusted p -value = 0.05/34 = 1.47E-03). Generally, in the brain, we identified that a total of 24 phenotypes belonging to cortical area were related to ERBB3, WNT4 and

CAMKV. A total of 40 phenotypes of cortical thickness were related to ERBB3, DPYD, TAB1, WNT4, and CLCN2. A total of ten phenotypes of cortical volume were related to ERBB3, DPYD, TAB1, WNT4, and CAMKV. While in the blood, only two genes, CYP2D6 and GDF11, were found genetically associated with cortical phenotypes. As for brain eQTL ERBB3, it was negatively associated with CA and CV of

some regions of the frontal lobe, temporal lobe, parietal lobe, and limbic system. Of note, genetically higher expression level of *ERBB3* in the brain was found negatively associated with CA of the right frontal pole (OR = 0.657, 95% CI 0.518–0.834, *p*-value = 5.61E-04, Fig. 5B), which is considered a control center of complex cognition. The elevated levels of *ERBB3* were genetically associated with both the CA and CV decline of pars orbitalis (left pars orbitalis CA: OR = 0.562, 95% CI 0.443–0.714, *p*-value = 2.23E-06; right pars orbitalis CA: OR = 0.633, 95% CI 0.498–0.803, *p*-value = 1.66E-04; left pars orbitalis CV: OR = 0.646, 95% CI 0.509–0.820, *p*-value = 3.23E-04, Fig. 5B). However, the causal relationship of *ERBB3* with CTH in cortical regions such as rostral middle frontal, superior parietal, inferior parietal, postcentral, precuneus, lateral occipital, rostral anterior cingulate, was found directionally opposite to that with CA and CV.

Blood eQTL *CYP2D6* was found positively associated with CA and CV of some regions of the frontal lobe and parietal lobe. Specifically, it was positively associated with left superior frontal CA (OR = 1.062, 95% CI 1.027–1.099, *p*-value = 4.67E-04), right superior parietal CA (OR = 1.061, 95% CI 1.026–1.098, *p*-value = 5.94E-04), right supramarginal CA (OR = 1.065, 95% CI 1.030–1.102, *p*-value = 2.61E-04), and right superior parietal CV (OR = 1.060, 95% CI 1.024–1.096, *p*-value = 8.41E-04).

The associations between candidate druggable genes and 16 imaging measures of subcortical volume were also evaluated (adjusted *p*-value = 0.05/8 = 6.25E-03). Brain eQTL *ERBB3* exerted negative effects on right putamen volume (OR = 0.699, 95% CI 0.551–0.887, *p*-value = 3.26E-03), while blood eQTL *CYP2D6* was negatively associated with left putamen volume (OR = 0.954, 95%

CI 0.922–0.987, *p*-value = 6.24E-03, Fig. 5B). The detailed results of candidate druggable genes and cortical and subcortical structure were shown in Table S14.

Association between candidate druggable genes and neurological diseases

Finally, the causal associations between candidate druggable genes and common neurological diseases were assessed (adjusted *p*-value = 0.05/23 = 2.17E-03). Our MR results revealed that increased *ATP2A1* and *WNT4* expression was associated with reduced risk of PD (*ATP2A1*: OR = 0.647, 95% CI 0.494–0.847, *p*-value = 1.52E-03; *WNT4*: OR = 0.613, 95% CI 0.468–0.804, *p*-value = 3.99E-04, Fig. 6A). Both blood and brain eQTLs of *ERBB3* had directionally consistent but suggestive effects on SAH, DLB, ALS, and epilepsy, among which ALS was further verified in the validation cohorts (Fig. 6B and Figure S4). In addition, *ERBB3* protein levels in the blood were found positively associated with LAS and migraine at the suggestive level (*p*-value < 0.05, Table S15). Furthermore, genetically predicted expression of *CYP2D6* was negatively associated with MS, MS severity, and migraine at the suggestive level (*p*-value < 0.05, Fig. 6A). The detailed results were shown in Table S15.

Steiger filtering analysis

Steiger filtering analysis was used to estimate the reliability of the causal direction between candidate druggable genes and cognitive function, brain structure, and neurological diseases. All candidate druggable genes passed Steiger filtering analysis, suggesting potential directional stability (*p*-value < 0.05, Table S16).

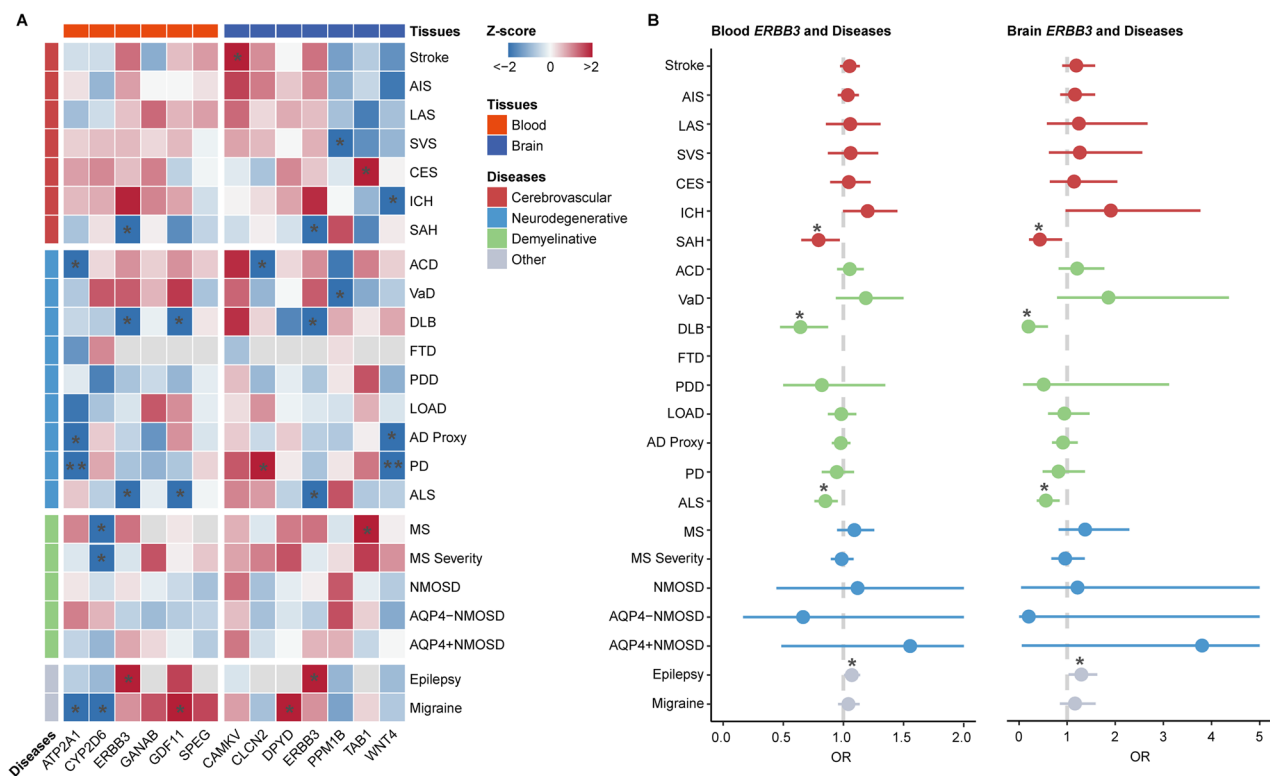


Fig. 6 Association between candidate druggable genes and neurological diseases. **A** Heatmap of associations between candidate druggable genes and common neurological diseases, which was presented by z-scores (**p*-value < 0.05, ***p*-value < 2.17E-03). **B** Forest plot for MR results between blood and brain eQTLs of *ERBB3* and neurological diseases (**p*-value < 0.05). ACD all-cause dementia, ALS amyotrophic lateral sclerosis, CES cardioembolic stroke, CI confidence interval, DLB dementia with Lewy bodies, eQTL expression quantitative trait loci, FTD frontotemporal dementia, ICH intracerebral hemorrhage, AIS acute ischemic stroke, LAS large artery atherosclerosis stroke, MS multiple sclerosis, NMOSD neuromyelitis optica spectrum disorder, OR odds ratio, PD Parkinson's disease, SVS small vessel stroke, SAH subarachnoid hemorrhage, SNP single nucleotide polymorphism, VaD vascular dementia.

Druggability of identified genes

We searched drug databases for candidate druggable genes identified in the MR analysis as possible drug targets. However, none of these were identified as drug targets for improving cognition, except *DPYD* (Table S17). Notably, several drugs targeting *DPYD* were also identified, one of which has been approved for a clinical trial to treat cognitive decline after major surgery. Drugs targeting *ERBB3* were primarily designed for treating cancers. No drug information was found for *TAB1*, *PPM1B*, *WNT4*, *ATP2A1*, *SPEG*, *GDF11*, or *CAMKV*.

DISCUSSION

In this study, we used eQTL data from blood and brain with GWAS data to investigate the causal relationships between 4302 druggable genes and cognitive performance, providing preclinical insights for drug development. MR and colocalization analyses provided evidence supporting causal relationships between candidate druggable genes and cognitive performance. Additionally, we endeavored to assess the causal effects of candidate druggable genes on brain structures and explore the potential mechanisms. We also explored the causal relationships between candidate genes and neurological disorders, aiming to develop targeted therapeutic approaches for improving cognitive function and delaying cognitive decline in various neurological conditions.

A prior study conducted by Lam et al. identified potential nootropic drug targets through GWAS and transcriptomic data [60]. On one hand, we replicated some of the findings from the previous study, such as the identification of *ERBB3*, *CYP2D6*, *GANAB*, *DPYD*, and *CLCN2* as genes associated with cognitive function. On the other hand, by combining MR and colocalization analyses, we identified several new genes potentially causally related to cognitive performance, including *SPEG*, *ATP2A1*, *GDF11*, *TAB1*, *WNT4*, *PPM1B*, and *CAMKV*. Furthermore, we expanded our analysis by exploring the genetic associations between candidate druggable genes and brain structure as well as neurological diseases, which provides further insight into how these genes may influence cognitive performance through their impact on brain health and neurological conditions.

Among candidate druggable genes that were causally associated with cognitive performance, we found that *ERBB3* is the one identified in both the brain and blood eQTL datasets. *ERBB3* encodes the ERBB3 receptor, which belongs to the epidermal growth factor receptor (EGFR) family, and is able to activate signaling pathways related to cell proliferation and differentiation by forming a heterodimer with ERBB2 or ERBB4 [61]. In the nervous system, neuregulins (NRG) serve as an EGFR ligand, binding to ERBB and contributing significantly to neural circuits assembly, myelin formation, and regulation of neurotransmission and synaptic plasticity [62, 63]. In line with this, our MR analysis suggested directionally consistent effects of *ERBB3* expression in both blood and brain on white matter phenotypes that reflect myelination, specifically manifesting as higher FA values and lower MD values in DTI. This causal relationship was further validated in the pQTL dataset. ERBB3 was associated with preserved white matter integrity in the corticospinal tract and parahippocampal part of cingulum. As for the other parts of the brain, we found that higher *ERBB3* expression has a causal relationship with the reduced subcortical volume of the putamen, reduced cortical surface area and volume, and increased cortical thickness of some regions. This discrepancy is speculated to be caused by the specific brain regions, as cortical thickness traits that are causally associated with *ERBB3* expression, are mainly located in the parietal lobes and occipital lobes, whereas cortical area and volume traits are primarily located in the frontal lobes, especially frontal pole, which is strongly associated with complex cognitive functions, and putamen is recently identified as one of the key brain structure linked to cognitive function in both genetic and

observational analyses [64]. As *ERBB3* was found to be negatively associated with cognitive performance on the level of gene and protein, we assume that the pathway through which *ERBB3* influences cognitive function might rely on its harm to the structure of the cortex and subcortex, despite its protective role in white matter microstructure. To unravel the complexities, further exploration of *ERBB3* expression in different brain structures is imperative. Furthermore, we demonstrated a protective relationship between *ERBB3* expression in both brain and blood and a set of neurologic diseases including SAH, DLB, ALS, and epilepsy, with ALS externally validated in ALS GWAS cohorts in Iacoangeli's study [65]. As ALS is a central nervous system neurodegenerative disease that exhibits white matter impairment in DTI [66], *ERBB3* may reduce the risk of ALS through its protection for white matter microstructure, extending its role in neurological diseases.

CYP2D6, which was found relevant to all the three categories of brain structure we analyzed, i.e. white matter, cortical and subcortical structures, encodes *CYP2D6* enzyme, a member of the cytochrome P450 family, and is predominantly expressed in the liver. According to data available in the World Guide for Drug Use and Pharmacogenomics and the EuroPharmaGenics (EPG) database, CYP enzymes engage in the metabolic pathways of 90% central nervous system drugs. Notably, *CYP2D6* participates in the metabolism of drugs employed to treat cognitive dysfunctions, such as donepezil, galantamine, and memantine [67]. Beyond effects on drug metabolism of anti-dementia drugs, our exploration of the genetic association between *CYP2D6* expression in the blood and cognitive performance revealed a significantly positive causal relationship. We also found that higher *CYP2D6* expression was causally associated with elevated FA values of left anterior thalamic radiation, and positively correlated with frontal and parietal cortical area and volume, suggesting that *CYP2D6* may enhance cognitive function by improving cortical and white matter structure. Moreover, increased *CYP2D6* expression was identified as having a mitigating effect on both susceptibility and severity of MS. As cognitive impairment comprises the manifestations of MS, with a prevalence of 63%, and the severity of cognitive impairment and MS is correlated [68], it is speculated that the pathways through which *CYP2D6* influences cognitive performance might go beyond brain structure. Future studies are warranted to explore these associations.

We also revealed that *PPM1B*, which encodes protein phosphatase Mg²⁺/Mn²⁺ dependent 1B, was negatively associated with cognitive performance. Consistently, higher expression level of *PPM1B* were associated with reduced subcortical volume in both sides of putamen and left caudate, which are the components of basal ganglia. As a functional entity, it connects the cortex, cerebellum and thalamus, participating in controlling autonomous movements as well as cognition. Taken together, *PPM1B* was assumed to influence cognitive performance through its harm to the volume of putamen and caudate, suggesting it a therapeutic target for enhancing cognitive function. As for the other candidate druggable genes, such as *GDF11*, *CLCN2*, *CAMKV*, *WNT4*, *DPYD* and *TAB1*, which were found to be associated with certain brain structures, their specific mechanisms underlying the association with cognitive performance require further investigation.

The strength of our study was the integration of MR and colocalization analyses to find novel therapeutic targets for cognitive performance. We have utilized eQTL data from both peripheral blood and brain to improve the robustness of the results and further evaluated their associations with brain health. Moreover, the MR results between *ERBB3* using eQTLs derived from blood and brain and cognitive performance were consistent and also repeated at the protein level. Compared with traditional drug discovery, the data-driven approach is able to discover candidate drug targets with high throughput but less time and money.

However, certain limitations to our study should be acknowledged. Firstly, almost all participants in the datasets were of European ancestry in this study. Consequently, the results of our analysis require validation in other ethnic groups. Second, considering the limited sample size in pQTL datasets and the absence of statistically significant SNPs, the validation of results at the protein level remains unfeasible. A comprehensive exploration of protein GWAS with a larger sample size is warranted for further investigation. Although our study utilized MR analysis to identify candidate druggable genes associated with enhanced cognitive function, experimental validation is crucial. Clinical trials are also essential to assess the efficacy and safety of interventions targeting these druggable genes concerning improving cognitive function. Lastly, the lack of GWAS data for distinct cognitive domains precludes the exploration of the causal relationships between candidate druggable genes and various cognitive domains. Furthermore, the associations between brain structure and diverse cognitive domains require further investigation.

CONCLUSIONS

Our integrative analysis provides genetic evidence supporting candidate therapeutic targets for improving cognitive performance and treating neurological diseases. Furthermore, it sheds light on the possible mechanisms by which these targets affect brain structures. This finding indicated that the identified druggable genes, particularly *ERBB3* and *CYP2D6*, have the potential to serve as targets for cognitive enhancement, though further validation is needed.

Data Sharing Statement

The GWAS data used in this study are publicly available. All the supporting data for the MR analyses are included in the article/Supplementary Material. Further inquiries can be directed to the corresponding authors.

CODE AVAILABILITY

This study used open-source software and codes, specifically R (<https://www.r-project.org/>), TwoSampleMR (<https://github.com/MRCIEU/TwoSampleMR>), and coloc (<https://chr1swallace.github.io/coloc/>).

REFERENCES

1. Roberts R, Knopman DS. Classification and epidemiology of MCI. *Clin Geriatr Med.* 2013;29:753–72.
2. Gauthier S, Reisberg B, Zaudig M, Petersen RC, Ritchie K, Broich K, et al. Mild cognitive impairment. *Lancet.* 2006;367:1262–70.
3. Plassman BL, Langa KM, Fisher GG, Heeringa SG, Weir DR, Ofstedal MB, et al. Prevalence of cognitive impairment without dementia in the United States. *Ann Intern Med.* 2008;148:427–34.
4. Eggers C, Arendt G, Hahn K, Husstedt IW, Maschke M, Neuen-Jacob E, et al. HIV-1-associated neurocognitive disorder: epidemiology, pathogenesis, diagnosis, and treatment. *J Neurol.* 2017;264:1715–27.
5. McCollum L, Karlawish J. Cognitive impairment evaluation and management. *Med Clin North Am.* 2020;104:807–25.
6. Yu T-W, Lane H-Y, Lin C-H. Novel therapeutic approaches for Alzheimer's disease: an updated review. *Int J Mol Sci.* 2021;22:8208.
7. Egan MF, Kost J, Voss T, Mukai Y, Aisen PS, Cummings JL, et al. Randomized trial of verubecestat for prodromal Alzheimer's disease. *N Engl J Med.* 2019;380:1408–20.
8. Panza F, Lozupone M, Seripa D, Imbimbo BP. Amyloid-β immunotherapy for Alzheimer disease: Is it now a long shot? *Ann Neurol.* 2019;85:303–15.
9. Mullard A. Failure of first anti-tau antibody in Alzheimer disease highlights risks of history repeating. *Nat Rev Drug Discov.* 2021;20:3–5.
10. Singh V, Chertkow H, Lerch JP, Evans AC, Dorr AE, Kabani NJ. Spatial patterns of cortical thinning in mild cognitive impairment and Alzheimer's disease. *Brain.* 2006;129:2885–93.
11. Yang J, Pan P, Song W, Huang R, Li J, Chen K, et al. Voxelwise meta-analysis of gray matter anomalies in Alzheimer's disease and mild cognitive impairment using anatomic likelihood estimation. *J Neurol Sci.* 2012;316:21–9.
12. Stahl R, Dietrich O, Teipel SJ, Hampel H, Reiser MF, Schoenberg SO. White matter damage in Alzheimer disease and mild cognitive impairment: assessment with diffusion-tensor MR imaging and parallel imaging techniques. *Radiology.* 2007;243:483–92.
13. Bozzali M, Falini A, Franceschi M, Cercignani M, Zuffi M, Scotti G, et al. White matter damage in Alzheimer's disease assessed *in vivo* using diffusion tensor magnetic resonance imaging. *J Neurol Neurosurg Psychiatry.* 2002;72:742–6.
14. Huo J, Zhang G, Wang W, Cao W, Wan M, Huang T, et al. Migraine and white matter lesions: a mendelian randomization study. *Sci Rep.* 2023;13:10984.
15. Smith EE, Salat DH, Jeng J, McCreary CR, Fischl B, Schmahmann JD, et al. Correlations between MRI white matter lesion location and executive function and episodic memory. *Neurology.* 2011;76:1492–9.
16. Berron D, van Westen D, Ossenkoppele R, Strandberg O, Hansson O. Medial temporal lobe connectivity and its associations with cognition in early Alzheimer's disease. *Brain.* 2020;143:1233–48.
17. Sekula P, Del Greco M F, Pattaro C, Köttgen A. Mendelian randomization as an approach to assess causality using observational data. *J Am Soc Nephrol.* 2016;27:3253–65.
18. Walker VM, Davey Smith G, Davies NM, Martin RM. Mendelian randomization: a novel approach for the prediction of adverse drug events and drug repurposing opportunities. *Int J Epidemiol.* 2017;46:2078–89.
19. Finan C, Gaulton A, Kruger FA, Lumbers RT, Shah T, Engmann J, et al. The druggable genome and support for target identification and validation in drug development. *Sci Transl Med.* 2017;9:eaag1166.
20. Storm CS, Kia DA, Almramhi MM, Bandres-Ciga S, Finan C, International Parkinson's Disease Genomics Consortium (IPDGC), et al. Finding genetically-supported drug targets for Parkinson's disease using Mendelian randomization of the druggable genome. *Nat Commun.* 2021;12:7342.
21. Zheng J, Zhang Y, Zhao H, Liu Y, Baird D, Karim MA, et al. Multi-ancestry Mendelian randomization of omics traits revealing drug targets of COVID-19 severity. *EBioMedicine.* 2022;81:104112.
22. Chen Y, Xu X, Wang L, Li K, Sun Y, Xiao L, et al. Genetic insights into therapeutic targets for aortic aneurysms: A Mendelian randomization study. *EBioMedicine.* 2022;83:104199.
23. Su W-M, Gu X-J, Dou M, Duan Q-Q, Jiang Z, Yin K-F, et al. Systematic druggable genome-wide Mendelian randomisation identifies therapeutic targets for Alzheimer's disease. *J Neurol Neurosurg Psychiatry.* 2023;94:954–61.
24. Võsa U, Claringbold A, Westra H-J, Bonder MJ, Deelen P, Zeng B, et al. Large-scale cis- and trans-eQTL analyses identify thousands of genetic loci and polygenic scores that regulate blood gene expression. *Nat Genet.* 2021;53:1300–10.
25. Wang D, Liu S, Warell J, Won H, Shi X, Navarro FCP, et al. Comprehensive functional genomic resource and integrative model for the human brain. *Science.* 2018;362:eaat8464.
26. Lawlor DA, Harbord RM, Sterne JAC, Timpson N, Davey Smith G. Mendelian randomization: using genes as instruments for making causal inferences in epidemiology. *Stat Med.* 2008;27:1133–63.
27. Sanderson E, Spiller W, Bowden J. Testing and correcting for weak and pleiotropic instruments in two-sample multivariable Mendelian randomization. *Stat Med.* 2021;40:5434–52.
28. Ferkingstad E, Sulem P, Atlaslon BA, Sveinbjörnsson G, Magnusson MI, Styrnisdottir EL, et al. Large-scale integration of the plasma proteome with genetics and disease. *Nat Genet.* 2021;53:1712–21.
29. Lee JJ, Wedow R, Okbay A, Kong E, Maghzian O, Zacher M, et al. Gene discovery and polygenic prediction from a genome-wide association study of educational attainment in 1.1 million individuals. *Nat Genet.* 2018;50:1112–21.
30. Hemani G, Zheng J, Elsworth B, Wade KH, Haberland V, Baird D, et al. The MR-Base platform supports systematic causal inference across the human genome. *Elife.* 2018;7:e34408.
31. Davies G, Marioni RE, Liewald DC, Hill WD, Hagenaars SP, Harris SE, et al. Genome-wide association study of cognitive functions and educational attainment in UK Biobank (N=112 151). *Mol Psychiatry.* 2016;21:758–67.
32. Davies G, Lam M, Harris SE, Trampush JW, Luciano M, Hill WD, et al. Study of 300,486 individuals identifies 148 independent genetic loci influencing general cognitive function. *Nat Commun.* 2018;9:2098.
33. Smith SM, Douaud G, Chen W, Hanayik T, Alfaro-Almagro F, Sharp K, et al. An expanded set of genome-wide association studies of brain imaging phenotypes in UK Biobank. *Nat Neurosci.* 2021;24:737–45.
34. Karlsgodt KH. White Matter Microstructure across the Psychosis Spectrum. *Trends Neurosci.* 2020;43:406–16.
35. Power MC, Su D, Wu A, Reid RI, Jack CR, Knopman DS, et al. Association of white matter microstructural integrity with cognition and dementia. *Neurobiol Aging.* 2019;83:63–72.
36. Ulivi L, Kanber B, Prados F, Davagnanam I, Merwick A, Chan E, et al. White matter integrity correlates with cognition and disease severity in Fabry disease. *Brain.* 2020;143:3331–42.

37. Malik R, Chauhan G, Taylor M, Sargurupremraj M, Okada Y, Mishra A, et al. Multiancestry genome-wide association study of 520,000 subjects identifies 32 loci associated with stroke and stroke subtypes. *Nat Genet*. 2018;50:524–37.
38. Kurki MI, Karjalainen J, Palta P, Sipilä TP, Kristiansson K, Donner KM, et al. FinnGen provides genetic insights from a well-phenotyped isolated population. *Nature*. 2023;613:508–18.
39. Chia R, Sabir MS, Bandres-Ciga S, Saez-Atienzar S, Reynolds RH, Gustavsson E, et al. Genome sequencing analysis identifies new loci associated with Lewy body dementia and provides insights into its genetic architecture. *Nat Genet*. 2021;53:294–303.
40. Van Deerlin VM, Sleiman PMA, Martinez-Lage M, Chen-Plotkin A, Wang L-S, Graff-Radford NR, et al. Common variants at 7p21 are associated with frontotemporal lobar degeneration with TDP-43 inclusions. *Nat Genet*. 2010;42:234–9.
41. Kunkle BW, Grenier-Boley B, Sims R, Bis JC, Damotte V, Naj AC, et al. Genetic meta-analysis of diagnosed Alzheimer’s disease identifies new risk loci and implicates A β , tau, immunity and lipid processing. *Nat Genet*. 2019;51:414–30.
42. Nalls MA, Blauwendraat C, Vallerga CL, Heilbron K, Bandres-Ciga S, Chang D, et al. Identification of novel risk loci, causal insights, and heritable risk for Parkinson’s disease: a meta-analysis of genome-wide association studies. *Lancet Neurol*. 2019;18:1091–102.
43. Nicolas A, Kenna KP, Renton AE, Ticozzi N, Faghri F, Chia R, et al. Genome-wide Analyses Identify KIF5A as a Novel ALS Gene. *Neuron*. 2018;97:1267–88.
44. Schwartzentruber J, Cooper S, Liu JZ, Barrio-Hernandez I, Bello E, Kumashita N, et al. Genome-wide meta-analysis, fine-mapping and integrative prioritization implicate new Alzheimer’s disease risk genes. *Nat Genet*. 2021;53:392–402.
45. International Multiple Sclerosis Genetics Consortium. Multiple sclerosis genomic map implicates peripheral immune cells and microglia in susceptibility. *Science*. 2019;365:eaav7188.
46. International Multiple Sclerosis Genetics Consortium, MultipleMS Consortium. Locus for severity implicates CNS resilience in progression of multiple sclerosis. *Nature*. 2023;619:323–31.
47. International League Against Epilepsy Consortium on Complex Epilepsies. Genome-wide mega-analysis identifies 16 loci and highlights diverse biological mechanisms in the common epilepsies. *Nat Commun*. 2018;9:5269.
48. Estrada K, Whelan CW, Zhao F, Bronson P, Handsaker RE, Sun C, et al. A whole-genome sequence study identifies genetic risk factors for neuromyelitis optica. *Nat Commun*. 2018;9:1929.
49. Sakaue S, Kanai M, Tanigawa Y, Karjalainen J, Kurki M, Koshiba S, et al. A cross-population atlas of genetic associations for 220 human phenotypes. *Nat Genet*. 2021;53:1415–24.
50. Mbatchou J, Barnard L, Backman J, Marcketta A, Kosmicki JA, Ziyatdinov A, et al. Computationally efficient whole-genome regression for quantitative and binary traits. *Nat Genet*. 2021;53:1097–103.
51. Kaivola K, Shah Z, Chia R, International LBD Genomics Consortium, Scholz SW. Genetic evaluation of dementia with Lewy bodies implicates distinct disease subgroups. *Brain*. 2022;145:1757–62.
52. Bowden J, Del Greco M F, Minelli C, Davey Smith G, Sheehan N, Thompson J. A framework for the investigation of pleiotropy in two-sample summary data Mendelian randomization. *Stat Med*. 2017;36:1783–802.
53. Bowden J, Davey Smith G, Haycock PC, Burgess S. Consistent estimation in mendelian randomization with some invalid instruments using a weighted median estimator. *Genet Epidemiol*. 2016;40:304–14.
54. Bowden J, Davey Smith G, Burgess S. Mendelian randomization with invalid instruments: effect estimation and bias detection through Egger regression. *Int J Epidemiol*. 2015;44:512–25.
55. Hartwig FP, Davey Smith G, Bowden J. Robust inference in summary data Mendelian randomization via the zero modal pleiotropy assumption. *Int J Epidemiol*. 2017;46:1985–98.
56. Hemani G, Tilling K, Davey Smith G. Orienting the causal relationship between imprecisely measured traits using GWAS summary data. *PLoS Genet*. 2017;13:e1007081.
57. Giambartolomei C, Vukcevic D, Schadt EE, Franke L, Hingorani AD, Wallace C, et al. Bayesian test for colocalisation between pairs of genetic association studies using summary statistics. *PLoS Genet*. 2014;10:e1004383.
58. Zuber V, Grinberg NF, Gill D, Manipur I, Slob EAW, Patel A, et al. Combining evidence from Mendelian randomization and colocalization: Review and comparison of approaches. *Am J Hum Genet*. 2022;109:767–82.
59. Wang K, Shi M, Huang C, Fan B, Luk AOY, Kong APS, et al. Evaluating the impact of glucokinase activation on risk of cardiovascular disease: a Mendelian randomisation analysis. *Cardiovasc Diabetol*. 2022;21:192.
60. Lam M, Chen C-Y, Ge T, Xia Y, Hill DW, Trampush JW, et al. Identifying nootropic drug targets via large-scale cognitive GWAS and transcriptomics. *Neuropharmacology*. 2021;46:1788–801.
61. Bublil EM, Yarden Y. The EGF receptor family: spearheading a merger of signaling and therapeutics. *Curr Opin Cell Biol*. 2007;19:124–34.
62. Mei L, Nave K-A. Neuregulin-ERBB signaling in the nervous system and neuropsychiatric diseases. *Neuron*. 2014;83:27–49.
63. Brinkmann BG, Agarwal A, Sereda MW, Garratt AN, Müller T, Wende H, et al. Neuregulin-1/ErbB signaling serves distinct functions in myelination of the peripheral and central nervous system. *Neuron*. 2008;59:581–95.
64. Siedlinski M, Carnevale L, Xu X, Carnevale D, Evangelou E, Caulfield MJ, et al. Genetic analyses identify brain structures related to cognitive impairment associated with elevated blood pressure. *Eur Heart J*. 2023;44:2114–25.
65. Iacoangeli A, Lin T, Al Khleifat A, Jones AR, Opie-Martin S, Coleman JRI, et al. Genome-wide Meta-analysis Finds the ACSL5-ZDHHC6 Locus Is Associated with ALS and Links Weight Loss to the Disease Genetics. *Cell Rep*. 2020;33:108323.
66. Iwata NK, Kwan JY, Danielian LE, Butman JA, Tovar-Moll F, Bayat E, et al. White matter alterations differ in primary lateral sclerosis and amyotrophic lateral sclerosis. *Brain*. 2011;134:2642–55.
67. Cacabelos R. Pharmacogenomics of cognitive dysfunction and neuropsychiatric disorders in dementia. *Int J Mol Sci*. 2020;21:3059.
68. Planche V, Gibelin M, Cregut D, Pereira B, Clavelou P. Cognitive impairment in a population-based study of patients with multiple sclerosis: differences between late relapsing-remitting, secondary progressive and primary progressive multiple sclerosis. *Eur J Neurol*. 2016;23:282–9.

ACKNOWLEDGEMENTS

The authors thank the studies or consortiums mentioned and included in the present analysis for providing public datasets. Some icons in Fig. 1 were created with BioRender and Servier Medical Art.

AUTHOR CONTRIBUTIONS

DST, CQ, LYZ, YXL conceived and designed the study. LYZ, YXL, YHC, and YFY analyzed and interpreted the data. LYZ and YXL drafted the manuscript. LQZ, SY, MHD, HZ, XWP, LC, LFZ, JX, KS, WW, CQ, and DST were involved in the supervision of the study. All authors contributed to the writing and approved the final version of the manuscript.

FUNDING

This study was supported by Ministry of Science and Technology China Brain Initiative Grant (2022ZD0204704), National Natural Science Foundation of China (Grants: 82371404, 82071380, 81873743, 82271341), Knowledge Innovation Program of Wuhan Shuguang Project (2022020801020454), and Tongji Hospital (HUST) Foundation for Excellent Young Scientist (Grant No. 2020YQ06).

COMPETING INTERESTS

The authors declared no potential conflicts of interest with respect to the research, authorship, and/or publication of this article.

ETHICS APPROVAL AND CONSENT TO PARTICIPATE

The data utilized in this study were obtained from publicly available databases. As this study did not involve direct research on human participants, animals, or identifiable images, no additional ethical approval was required. All original studies related to databases obtained the necessary ethical approval and informed consent from participants. All methods were performed in accordance with relevant guidelines and regulations.

ADDITIONAL INFORMATION

Supplementary information The online version contains supplementary material available at <https://doi.org/10.1038/s41398-025-03437-w>.

Correspondence and requests for materials should be addressed to Chuan Qin or Dai-Shi Tian.

Reprints and permission information is available at <http://www.nature.com/reprints>

Publisher’s note Springer Nature remains neutral with regard to jurisdictional claims in published maps and institutional affiliations.



Open Access This article is licensed under a Creative Commons Attribution-NonCommercial-NoDerivatives 4.0 International License, which permits any non-commercial use, sharing, distribution and reproduction in any medium or format, as long as you give appropriate credit to the original author(s) and the source, provide a link to the Creative Commons licence, and indicate if you modified the licensed material. You do not have permission under this licence to share adapted material derived from this article or parts of it. The images or other third party material in this article are included in the article's Creative Commons licence, unless indicated otherwise in a credit line to the material. If material is not included in the article's Creative Commons licence and your intended use is not permitted by statutory regulation or exceeds the permitted use, you will need to obtain permission directly from the copyright holder. To view a copy of this licence, visit <http://creativecommons.org/licenses/by-nc-nd/4.0/>.

© The Author(s) 2025